Available online at www.sciencedirect.com
ScienceDirect
Acta Materialia 58 (2010) 3422–3428
Acta MATERIALIA
www.elsevier.com/locate/actamat

Thermodynamic evaluation of hypereutectic Al–Si (A390) alloy with addition of Mg

Alireza Hekmat-Ardakan, Frank Ajersch *

École Polytechnique de Montréal, Dép. de Génie Chimique, P.O. Box 6079, Centre-Ville, Montreal, Quebec, Canada H3C 3A7

Received 1 June 2009; received in revised form 9 February 2010; accepted 9 February 2010
Available online 10 March 2010

Abstract

This paper presents the thermodynamic evaluation of A390 hypereutectic Al–Si alloy (Al–17% Si–4.5% Cu–0.5% Mg) and alloys up to 10% Mg, using the Factsage® software. Two critical compositions were detected at 4.2% and 7.2% Mg where the temperatures of the liquidus, the start of the binary and of the ternary eutectic reaction are changed. These critical compositions show differences in the formation of Mg_2Si intermetallic particles during the solidification interval. For compositions up to 4.2% Mg, the Mg_2Si intermetallic phase first appears in the ternary eutectic zone. With Mg contents between 4.2% and 7.2%, Mg_2Si particle appears in both the binary and ternary eutectic reactions. Above 7.2% Mg, it solidifies as a primary phase and also during the binary and ternary reactions. The calculated liquid fraction vs. temperature curves also showed a decrease of the eutectic formation temperature (knee point temperature) with the addition of Mg content up to 4.2% Mg. This temperature becomes almost constant up to 10% Mg. The calculation of eutectic formation temperature shows a good agreement with differential scanning calorimetry (DSC) tests.

Keywords: Thermodynamic; Factsage; Aluminum alloys; Eutectic solidification; Magnesium

1. Introduction

Hypereutectic Al–Si alloys such as A390 (Al–17% Si–4.5% Cu–0.5% Mg) are used in applications that require high resistance to wear and corrosion, good mechanical properties, low thermal expansion and reduced density. These properties are of particular interest to the automobile industry for the production of fuel-efficient vehicles using light-weight components produced from these alloys such as connecting rods, pistons, air conditioner compressors, cylinder liners and engine blocks [1]. Their good mechanical properties and high resistance to wear are essentially attributed to the presence of hard primary silicon particles distributed in the matrix. Therefore, the size and morphology of primary silicon in hypereutectic Al–Si alloys influence the mechanical properties of the alloys. However, the mechanical properties of hypereutectic Al–Si alloys such as A390 alloy have not been optimized due to the large size of primary Si particles which restricts the application of this alloy. During service conditions, cracks can nucleate on the large primary silicon particles where the resultant stress concentration at the interface between these particles and the matrix will be more severe relative to those between fine Si phases and the matrix [2]. It has been shown that Mg_2Si/Al–Si composites have a high potential for wear resistance applications similar to Si/Al–Si composites, because the intermetallic compound Mg_2Si also exhibits a high melting temperature, low density, high hardness, low thermal expansion coefficient, equilibrium interface and excellent workability with a potential for cost reduction [3]. Similarities exist between Mg_2Si and Si in terms of properties and solidification behaviour [4]. The most important advantage is the possibility of producing lighter components due to the lower density of Mg_2Si (1.99 g cm^{-3}) compared to Si (2.33 g cm^{-3}) which can contribute to the light weighting of the vehicles [5].

* Corresponding author. Tel.: +1 514 340 4711x4533; fax: +1 514 340 4468.
E-mail address: frank.ajersch@polymtl.ca (F. Ajersch).

1359-6454/$36.00 © 2010 Acta Materialia Inc. Published by Elsevier Ltd. All rights reserved.
doi:10.1016/j.actamat.2010.02.017

2. Methodology

To better understand the solidification behaviour and compound formation of alloys with higher Mg content, an investigation of the thermodynamic properties and the solidification behaviour was carried out using the Factsage® software developed by the CRCT group at Ecole Polytechnique de Montreal using the Fslite (Factsage® light metal alloy database) database. The FactSage's FSlite light alloy database was derived from the European COST Action 507 (COST 507, Thermochemical database for light metal alloys) [6]. The calculations were carried out assuming a quaternary system (Al–Si–Cu–Mg) with a constant composition (isopleth) of 4.5% Cu and 17% silicon and with Mg/Al ratios of 0.5/78 to 10/68.5 representing 0.5–10% Mg contents, respectively. All compositions and solid fractions are given in weight percent (wt.%) unless otherwise stated. Commercial A390 alloy normally contains other elements such as Mn, Ni, Pb, Sn, Sr, Ti, Zn. These constituents are minor and are generally less than 0.02% and are not included in the thermodynamic analysis. The content of theses elements is sufficiently low and would not change the phase diagram to any significant extent.

The eutectic microstructure of commercial A390 alloy (Al–17.4% Si–4.58% Cu–0.58% Mg–0.32% Fe–0.02% Mn–0.02% Ti–0.0003% P) and experimental alloys with additions of Mg were investigated using scanning electron microscopy (SEM). The high Mg content alloys were produced by adding AZ91Mg-base alloy (Mg–9.3% Al–0.12% Mn–0.62% Zn–0.02% Si) to A390 alloy. The alloys were conventionally cooled from the liquid state contained in a graphite crucible with cooling rate of $-0.15 \pm 0.05\ ^{\circ}C\ s^{-1}$, using a temperature controlled electric resistance furnace.

Duplicate differential scanning calorimetry (DSC) measurements were also carried out for commercial A390 alloy and alloys with addition of 6% and 10% Mg at a cooling rate of $0.15\ ^{\circ}C\ s^{-1}$ using a TG analyzer (Model: Setsys 16/18, SETARAM). The measured temperatures were compared to the calculated values using the Factsage® software.

3. Results and discussion

3.1. Thermodynamic predictions

Fig. 1 shows the calculated isopleth phase diagram of the basic A390 alloy of composition Al–17% Si–4.5% Cu–0.5% Mg without trace elements. The dashed line at 17% Si indicates the temperature regions of the formation of primary Si as well as the binary, ternary and quaternary reactions that occur at transition temperatures of 653.1, 566.2, 502.4 and 496.9 °C, respectively. The calculations confirm that the Si starts to precipitate as a primary phase from the liquid phase at 653.1 °C and continues to precipitate to 566.2 °C, with a maximum solid fraction of 6.1%. At this point, which is also called "knee" point, a dendritic network of α-Al and eutectic Si starts to form and continues to solidify down to 502.4 °C. Between these two temperatures, 88% of the liquid phase changes to form the solid network. The ternary reaction takes place below this temperature to form Mg_2Si:

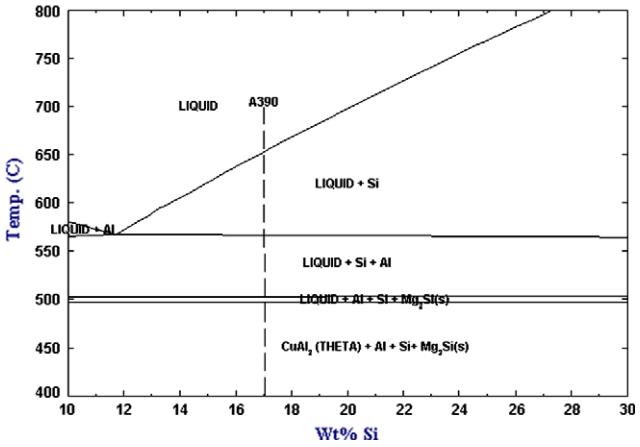

Fig. 1. Isopleth of the Al–Si–4.5% Cu–0.5% Mg system (basic A390 alloy). The dashed line represents the composition of A390 alloy at 17% Si calculated by Factsage®.

$$\text{Liq.} \rightarrow \text{Al} + \text{Si} + \text{Mg}_2\text{Si} \quad (1)$$

This ternary eutectic zone is very small and continues down to the temperature of 496.9 °C where only 2.0% of the remaining liquid changes to form the ternary phases. The solidification becomes complete with a quaternary reaction where the last remaining liquid (3.9%) solidifies corresponding to Reaction (2) as follows:

$$\text{Liq.} \rightarrow \text{CuAl}_2 + \text{Al} + \text{Si} + \text{Mg}_2\text{Si} \quad (2)$$

Other studies [7–10], have reported that the quaternary reaction proceeds according to the following reaction forming an additional solid phase:

$$\text{Liq.} \rightarrow \text{CuAl}_2 + \text{Al} + \text{Si} + \text{Cu}_2\text{Mg}_8\text{Si}_6\text{Al}_5 \quad (3)$$

The quaternary compound, $Cu_2Mg_8Si_6Al_5$ called the Q phase, is not included in the Factsage® database and is therefore not considered in the calculated diagram. However, microstructural observation identifies the presence of the $Cu_2Mg_8Si_6Al_5$ phase which is associated with $CuAl_2$ (θ phase) in the solidified microstructure [10,11]. Also, Mg_2Si has not been observed by other studies implying that any Mg_2Si can also be transformed to the Q phase according to the following reaction [12]:

$$\text{Liq.} + \text{Mg}_2\text{Si} \rightarrow \text{CuAl}_2 + \text{Al} + \text{Si} + \text{Cu}_2\text{Mg}_8\text{Si}_6\text{Al}_5 \quad (4)$$

According to Backerud et al. [12], Reactions (1), (4), and (3) occur at 555 °C, 512 °C and 507 °C, respectively. A considerable discrepancy is observed between the Factsage® calculation and the results of Backerud et al. [12] for predicting the temperature of Reaction (1). The main reason for this discrepancy is due to Reaction (4), which is not taken into account by FactSage® because the software does not include the basic thermodynamic data for Cu_2Mg_8-

Si_6Al_5 (Q phase). Reaction (4) indicates that Q phase is formed by the reaction of Mg_2Si and the liquid phase. Consequently, small solid fraction of Mg_2Si remains at the end of the solidification. If Reaction (4) is not considered, the Factsage® calculation shows that the Reaction (1) should occur at a lower temperature, near the end of the solidification at 502.4 °C, rather than at 555 °C as shown by Ref. [12] in order to keep the solid fraction of Mg_2Si as low as possible. This discrepancy is more pronounced for A390 than for the alloys with higher Mg content where Reaction (1) predominates the Mg_2Si precipitation. Factsage® calculations show predicts that the temperature of Reaction (1) increases abruptly from 502.4 °C to 526.6 °C when the Mg content increases from 0.5% to 1%.

Table 1 shows the calculated liquid fraction, the compositions as well as the solid fraction (%) of each solid constituent during the transformation reactions of the basic A390 alloy. It should be noted that the binary and ternary reactions take place at the temperature intervals between 566.2–502.4 °C (binary) and 502.4–496.9 °C (ternary), respectively. However the quaternary reaction occurs at an isothermal temperature of 496.9 °C at the final stage of solidification. The binary reaction has the largest contribution in forming solid phases Al + Si (88.0%) whereas the ternary reaction has a much smaller contribution (2.0%) in forming Al + Si + Mg_2Si phases. The microstructure of the solidified eutectic therefore consists of a dendritic network where the predominant phases observed are Al + Si.

The liquid and solid phase fractions of each constituent solidified under equilibrium conditions are also shown in Fig. 2 for the basic four component A390 alloy. It can be observed that the liquid fraction decreases slowly down to 566.2 °C (knee point) during the precipitation of primary silicon. With decreasing temperature the liquid fraction decreases rapidly down to 502.4 °C where the ternary reaction occurs. This reaction does not have a significant effect on the liquid fraction curve as previously indicated. Finally, the solidification becomes complete at the isothermal quaternary reaction. This figure also indicates that the main intermetallic phase in the microstructure at this stage is $CuAl_2$ (θ). These diagrams are calculated for equilibrium conditions, where the cooling rate is slow enough to include diffusion in the solid state throughout the solidification. The final phases will therefore consist of solids of a composition corresponding to the end of the eutectic temperature tie line and liquid of

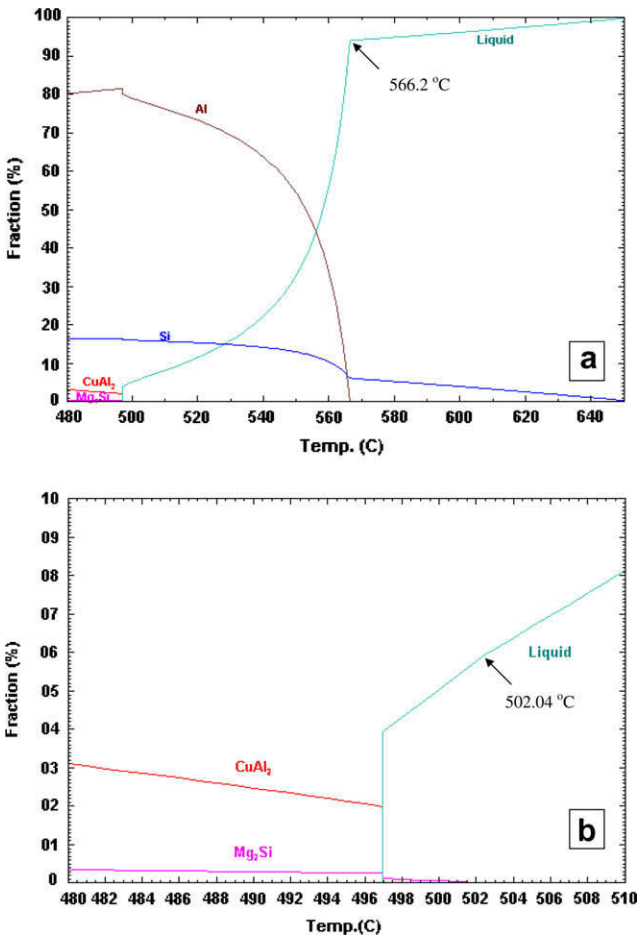

Fig. 2. The variation of liquid fractions and other solidified phases with temperature in the solidification interval for the basic A390 alloy (a), detailed diagram at high solid fraction (b).

eutectic composition [13]. Fig. 3 compares the liquid fraction of the basic A390 alloy for equilibrium and Scheil solidification where there is no diffusion in the solid phase. The Scheil and equilibrium curves are coincident for liquid fractions up to about 50%. However, for values less than 50% liquid, the equilibrium curve results in a smaller amount of liquid at a given temperature. The calculations show a significant decrease of solid fraction at the quaternary eutectic temperature. At the equilibrium condition the solidification rate becomes more pronounced due to the diffusion effect in solid. This is valid only for very slow rates of temperature decreases. For non-equilibrium cooling,

Table 1
The liquid and solid fractions for basic A390 alloy transition reactions.

Reactions	A390	Liquid fraction (%)	Liquid composition (wt.%)				Solid fraction (%)	Constituent percentage (wt.%)			
	Temperature (°C)		Al	Si	Cu	Mg		Al	Si	θ^a	Mg_2Si
Primary Si	653.1	100	78	17	4.5	0.5	0	–	–	–	–
Start of binary	566.2	93.9	83.0	11.6	4.9	0.5	6.1	–	100	–	–
Start of ternary	502.4	5.9	62.8	7.5	27.1	2.6	94.1	83.2	16.8	–	–
Quaternary	496.9	3.9	61.5	7.2	28.9	2.4	96.1	83.1	16.7	–	0.2
	496.9–δT	0	–	–	–	–	100	81.4	16.2	2.1	0.3

[a] $\theta = CuAl_2$.

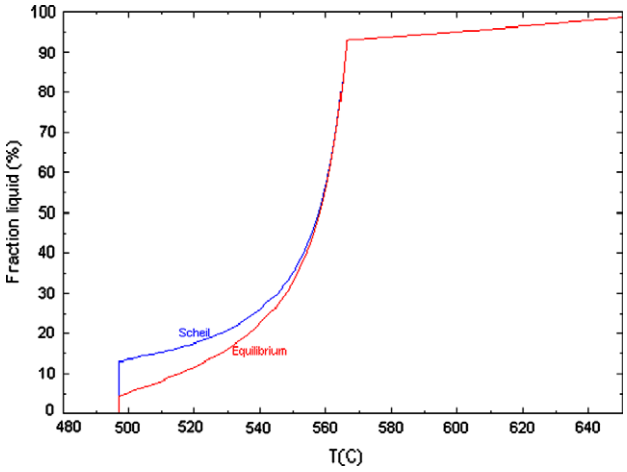

Fig. 3. The liquid fractions vs. temperature for the basic A390 alloy for equilibrium and Scheil (no-diffusion) conditions.

Table 2
Comparison of the weight percent of the intermetallic phases $CuAl_2$ and Mg_2Si solidified at the equilibrium and the Scheil cooling condition calculated by Factsage®.

Cooling condition	Phases	
	$CuAl_2$ (%)	Mg_2Si (%)
Equilibrium	2.1	0.3
Scheil	6.66	0.6

more liquid is present during the final stage of solidification compared to the case of equilibrium cooling. This results in a microstructure showing precipitation of more intermetallic compounds such as $CuAl_2$, when compared to the equilibrium condition, as shown in Table 2.

With higher Mg content, the calculations showed two compositions of Mg, at 4.2% and at 7.2%, that demonstrate critical transitions. The transition temperatures, including the liquidus, the start of binary and the ternary eutectic reactions were determined at these critical points. Table 3

Table 3
Effect of Mg variation on the formation temperatures.

% Mg	$T_{Liquidus}$ (°C)	Start of binary reaction, T (°C)	Start of ternary reaction, T (°C)	Quaternary reaction temperature, T (°C)
0.5[a]	653.1	566.2	502.4	496.9
1	649.7	564.0	526.6	496.9
2	642.8	559.6	541.4	496.9
3	635.7	555.2	546.7	496.9
4	628.4	551.0	549.3	496.9
4.2[b]	626.9	550.2	549.7	496.9
5	620.9	565.8	549.8	496.9
6	613.2	584.6	549.7	496.9
7	605.4	600.7	549.6	496.9
7.2[c]	603.8	603.7	549.6	496.9
8	617.0	599.8	549.5	496.9
9	632.2	594.5	549.3	496.9
10	646.1	588.9	549.2	496.9

[a] A390 composition.
[b] First critical point.
[c] Second critical point.

shows the temperature differences for variable Mg contents, compared to the basic A390 alloy. The liquidus temperature decreases from 653.1 °C (0.5% Mg) to 626.9 (4.2% Mg), continues to decrease to 603.8 °C (7.2% Mg) and then increases to 646.1 °C (10% Mg). The binary reaction temperature initially decreases from 566.2 °C to 550.2 °C for 4.2% Mg, increasing to 603.7 °C for 7.2% Mg and then decreases again to 588.9 °C at 10% Mg. The ternary reaction temperature increases gradually from 502.4 °C (0.5% Mg) to 549.7 °C (4.2% Mg) and then becomes almost constant with further increase in Mg content. The variation of the Mg content has no effect on the isothermal quaternary reaction temperature (solidus). Fig. 4 graphically demonstrates the variation of the transition temperatures as a function of Mg content illustrating the two critical Mg points at 4.2% and 7.2%.

These two critical Mg points can be also defined by considering the temperature range of formation of Mg_2Si intermetallic particles during the solidification interval, as shown in the shaded zone of Fig. 4. With the addition of Mg, the Mg_2Si intermetallic phase first appears only in the ternary eutectic zone. With Mg contents between 4.2% and 7.2%, solid Mg_2Si appears in the both binary and ternary reactions. Above 7.2% Mg, it solidifies as a primary phase as well as during the binary and ternary eutectic reactions. This implies that the formation range of Mg_2Si intermetallic particles can be significantly increased with the addition of Mg.

Table 4 shows the liquid fraction and the compositions at the transition temperatures as well as the solid fraction with the percentage of each solid constituent for a 10% Mg alloy. The calculated results indicate that the solidification starts with the precipitation of Mg_2Si from the liquid. Subsequently, the pro-eutectic silicon solidifies along with

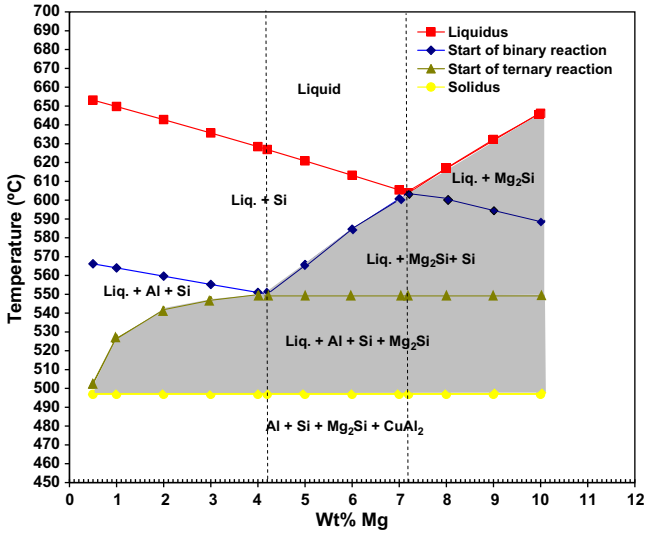

Fig. 4. The effect of Mg content on the transition reactions and corresponding temperatures for Al–17% Si–4.5% Cu alloys. Critical points occur at 4.2% and 7.2% Mg. The shaded zone shows the solidification interval of Mg_2Si intermetallic phase for different Mg contents.

Table 4
The liquid and solid fractions for A390 + 10% Mg alloy transition reactions.

Reactions	A390 + 10% Mg	Liquid fraction (%)	Liquid composition (wt.%)				Solid fraction (%)	Constituent percentage (wt.%)			
	Temperature (°C)		Al	Si	Cu	Mg		Al	Si	θ^a	Mg_2Si
Primary Mg_2Si	646.1	100	68.5	17	4.5	10	0	–	–	–	–
Start of binary	588.9	93.6	73.1	15.6	4.8	6.5	6.3	–	–	–	100
Start of ternary	549.2	87.8	77.9	12.4	5.1	4.6	12.2	–	21.2	–	78.8
Quaternary	496.9	5.5	61.5	7.1	28.9	2.5	94.5	72.8	11.2	–	16
	496.9−δT	0	–	–	–	–	100	71.1	10.8	2.8	15.3

[a] $\theta = CuAl_2$.

the Mg_2Si down to the eutectic formation temperature of 549.2 °C. At this point the eutectic network starts to form according to the ternary eutectic reaction. The values of the calculated liquid fraction demonstrate that 82.3% of the liquid phase is transformed to ternary eutectic phases (Al, Si and Mg_2Si) and the resulting eutectic solidification structure for high Mg content alloys corresponds to the ternary reaction.

Fig. 5 shows the liquid and solid phase fractions of each constituent in the solidification interval of a 10% Mg alloy. The solidification rates of Si and Mg_2Si during solidification interval are very similar. Zhang et al. [4] have also shown that the binary Al–Si and quasi-ternary Al–Mg_2Si systems are very similar, where growth rates are characterized by the faceted structure of the primary phases and the non-faceted eutectic phase. Fig. 6 compares the liquid fraction vs. temperature curves of the basic A390, 6% Mg and 10% Mg alloys according to Scheil solidification. It can be clearly observed that the eutectic formation temperature, corresponding to the knee point, significantly decreases from 566.2 °C to 549.7 °C when the Mg content reaches 6%. Almost identical values of the eutectic formation temperature were calculated for 6% and 10% Mg content. Fig. 7 indicates that this temperature decreases rapidly up to 4.2% Mg (first critical Mg point) and becomes nearly constant at 549 °C.

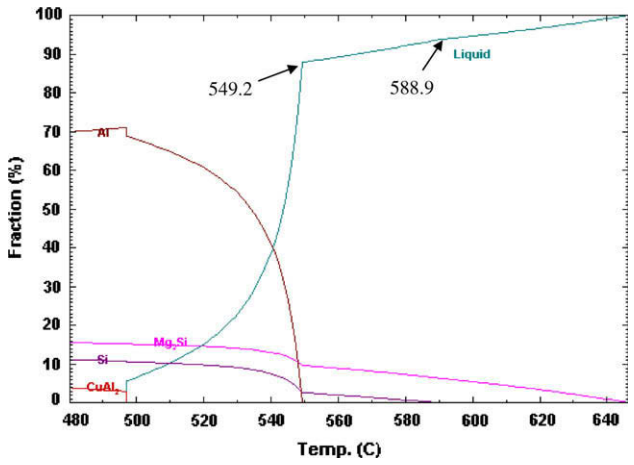

Fig. 5. Fraction of liquid and other phases solidified in the solidification interval vs. temperature for 10% Mg alloy.

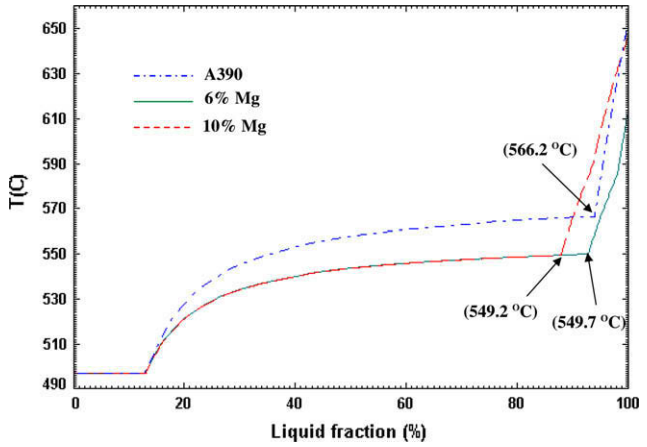

Fig. 6. Comparison of the liquid fraction vs. temperature curves for basic A390, 6% Mg and 10% Mg alloys during the solidification interval according to Scheil solidification.

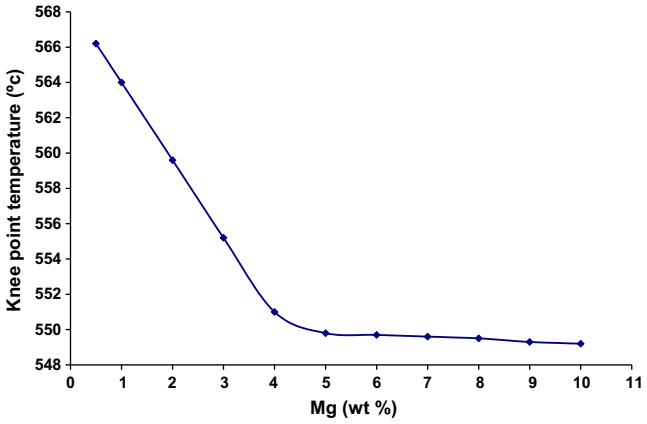

Fig. 7. The variation of knee point temperature of alloys with increasing the Mg content calculated using Factsage®.

3.2. DSC measurements and microstructural observation

Fig. 8 shows the result of DSC test carried out for commercial A390 alloy and for alloys with 6% and 10% Mg. Fig. 8a shows that the measured temperature of Reactions (1), (4), and (3) occur for A390 alloy at 538.2, 505.2 and 499.6 °C, respectively. Other studies have also shown similar results for the transition temperatures of A390 alloy using thermal analysis [14,15]. Fig. 8b and c shows the

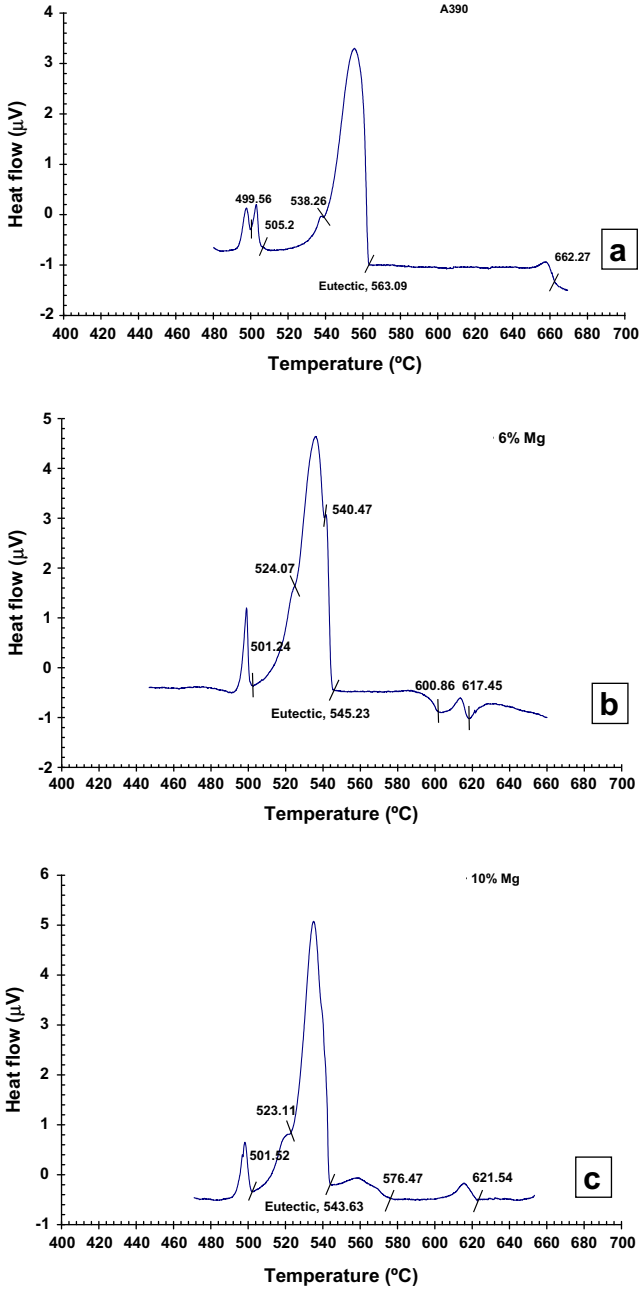

Fig. 8. DSC results of commercial A390 alloy (a) and alloys with 6% Mg (b) and 10% Mg (c) for a cooling rate of 0.15 °C s^{-1}.

results of DSC test for the 6% Mg and 10% Mg alloys carried out in this study.

The DSC tests indicate that the eutectic formation temperature at the knee point for A390 alloy decreases abruptly with increasing Mg up to 6% Mg content and then becomes more gradual with a further increase in Mg, as predicted by Factsage® calculation (Figs. 6 and 7). The decrease of the eutectic formation temperature has been shown to have a direct effect on the number of potential nuclei of eutectic Si found in the melt [16]. There are fewer barriers for nucleation with increasing nucleation temperature and thus a greater number of isolated eutectic Si particles may form. It is therefore anticipated that the reduction of the knee point temperature with increasing Mg content can modify the morphology of the eutectic silicon phase.

Fig. 9 shows the eutectic microstructure of A390 alloy and that of alloys with 6% Mg for conventionally cooled samples, using scanning electron microscopy (SEM). This figure indicates that the eutectic reaction changes with the addition of Mg from a binary (Al + Si) to a ternary (Al + Si + Mg_2Si) reaction, as predicated. The morphology of eutectic silicon distributed in matrix microstructure also changes significantly with Mg content from large individual flakes (Fig. 9a) to a fine network, similar to that of the eutectic Mg_2Si which presents itself in a Chinese script morphology (Fig. 9b). The change in eutectic silicon with addition of Mg is attributed to both the decrease in the temperature of eutectic formation and the change in the nature of eutectic reaction from binary to ternary.

4. Conclusions

Thermodynamic computations using FactSage® have shown that the solidification of basic A390 (Al–17% Si–4.5% Cu–0.5% Mg) alloy proceeds sequentially where the primary, binary, ternary and quaternary reactions occur at temperatures of 653.1, 566.2, 502.4 and 496.9 °C, respectively. With hypereutectic alloys up to 10% Mg, two critical compositions were detected at 4.2% and 7.2% Mg where

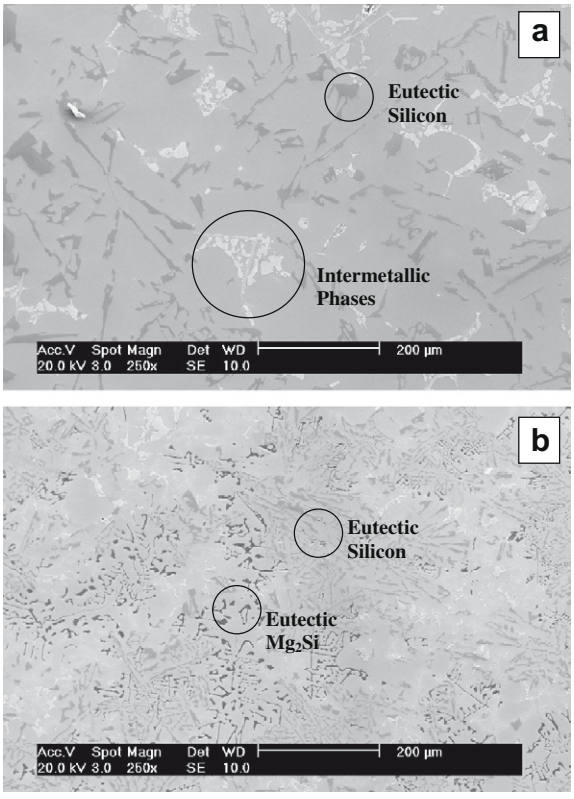

Fig. 9. SEM micrograph of the eutectic microstructure of (a) A390 alloy and (b) alloy with addition of 6% Mg content from conventionally cooled samples.

the formation temperatures for the liquidus, the start of the binary and of the ternary eutectic reaction are changed. These variations are also defined by the temperature range of the formation of Mg_2Si intermetallic particles. The Mg_2Si intermetallic phase first appears only in the ternary eutectic zone for composition up to 4.2% Mg. With Mg contents between 4.2% and 7.2%, Mg_2Si is produced in both the binary and the ternary reactions. Above 7.2% Mg, it solidifies as a primary phase as well as during the binary and ternary reactions. The solidified microstructure of the basic A390 alloy corresponds to the binary eutectic structure of Al + Si, whereas for alloys with Mg contents greater than 4.2%, a solidified ternary structure of Al + Si + Mg_2Si is formed.

The liquid fraction vs. temperature curves for the solidification of the basic A390, 6% Mg and 10% Mg alloys, calculated according to the Scheil equation, indicate that the eutectic formation temperature (knee point) for the 6% Mg and 10% Mg alloys occur at the same temperature of 549 °C. This is 17 °C lower than the eutectic formation temperature of A390 alloy at 566 °C and results in modification of eutectic Si in the matrix.

Acknowledgments

The authors gratefully acknowledge the financial support from the Fonds Quebecois de Recherche sur la Nature et les Technologies (FQRNT) and Natural Sciences and Engineering Research Council (NSERC) of Canada. The authors thank Prof. Arthur D. Pelton, Director of the research center of CRCT (Centre for Research in Computational Thermochemistry) for constructive suggestions about Factsage®.

References

[1] Lasa L, Rodriguez-Ibab JM. Mater Sci Eng A 2003;363:193.
[2] Feng Wang, Ma Yajun, Zhang Zhengye, Cui Xiaohao, Jin Yuansheng. Wear 2004;256:342.
[3] Zhao YG, Qin QD, Zhao YQ, Liang YH, Jiang QC. Mater Lett 2004;58:2192.
[4] Zhang J, Fan Z, Wang YQ, Zhou BL. Mater Sci Eng A 2000;281:104.
[5] Qin QD, Zhao YG, Zhou W. Wear 2008;264:654.
[6] Bale Christopher W, Pelton Arthur D. FACTSAGE 5.4.1, C.R.C.T (Centre of Research for Computational Thermochemistry). École Polytechnique de Montréal. <http://www.crct.polymtl.ca>.
[7] Mondolfo LF. Manganese in aluminum alloys. USA: Syracuse University, The Centre; 1978.
[8] Kapranos P, Kirkwood DH, Atkinson HV, Rheinlander JT, Bentzen JJ, Toft PT, et al. J Mater Process Technol 2003;135:271.
[9] Lasa L, Rodriguez-Ibabe JM. Mater Charact 2002;48:371.
[10] Li Jian, Elmadagli M, Gertsman VY, Lo J, Alpas AT. Mater Sci Eng A 2006;421:317.
[11] Elmadagli M, Alpas AT. Wear 2006;261:367.
[12] Backerud Lennart, Chai GuoCai, Tamminen Jarmo. Solidification characteristics of aluminum alloys, vol. 2. Sweden: University of Stockholm, Amer Foundry Society; 1993.
[13] Liu D, Atkinson HV, Jones H. Acta Mater 2005;53:3807.
[14] Birol Yücel. J Mater Process Technol 2008;207:200.
[15] Robles Hernández FC, Sokolowski JH. J Alloys Compd 2006;426:205.
[16] Nafisi S, Ghomashchi R. Mater Sci Eng A 2006;415:273.